



HAL
open science

Global analysis of aerosol properties above clouds

F. Waquet, F. Peers, F. Ducos, P. Goloub, S. Platnick, J. Riedi, D. Tanré, F. Thieuleux

► **To cite this version:**

F. Waquet, F. Peers, F. Ducos, P. Goloub, S. Platnick, et al.. Global analysis of aerosol properties above clouds. *Geophysical Research Letters*, 2013, 40, pp.5809-5814. 10.1002/2013GL057482 . insu-03620880

HAL Id: insu-03620880

<https://insu.hal.science/insu-03620880>

Submitted on 27 Mar 2022

HAL is a multi-disciplinary open access archive for the deposit and dissemination of scientific research documents, whether they are published or not. The documents may come from teaching and research institutions in France or abroad, or from public or private research centers.

L'archive ouverte pluridisciplinaire **HAL**, est destinée au dépôt et à la diffusion de documents scientifiques de niveau recherche, publiés ou non, émanant des établissements d'enseignement et de recherche français ou étrangers, des laboratoires publics ou privés.

Copyright

Global analysis of aerosol properties above clouds

F. Waquet,¹ F. Peers,¹ F. Ducos,¹ P. Goloub,¹ S. Platnick,² J. Riedi,¹ D. Tanré,¹ and F. Thieuleux¹

Received 26 July 2013; revised 30 September 2013; accepted 9 October 2013; published 14 November 2013.

[1] The seasonal and spatial variability of Aerosol Above Cloud (AAC) properties are derived from passive satellite data for the year 2008. A significant amount of aerosols are transported above liquid water clouds on the global scale. For particles in the fine mode (i.e., radius smaller than 0.3 μm), including both clear-sky and AAC, retrievals increase the global mean aerosol optical thickness by 25(\pm 6)%. The two main regions of originated anthropogenic AAC are the tropical Southeast Atlantic, for biomass-burning aerosols, and the North Pacific, mainly for pollutants. Man-made AAC are also detected over the Arctic during the spring. Mineral dust particles are detected above clouds within the so-called “dust belt” region (5–40° N). AAC may cause a warming effect and bias the retrieval of the cloud properties. This study will then help to better quantify the impacts of aerosols on clouds and climate. **Citation:** Waquet, F., F. Peers, F. Ducos, P. Goloub, S. Platnick, J. Riedi, D. Tanré, and F. Thieuleux (2013), Global analysis of aerosol properties above clouds, *Geophys. Res. Lett.*, 40, 5809–5814, doi:10.1002/2013GL057482.

1. Introduction

[2] Aerosols play a major role in the Earth’s climate system through their interactions with solar radiation (direct effect), their influence on cloud properties (indirect and semidirect effects) and the hydrological cycle [Ramanathan *et al.*, 2001]. Their negative forcing (cooling effect) may partially compensate for greenhouse gas effects. However, the radiative forcing due to both direct and indirect effects remains a large source of uncertainty. On the positive side, continuous global satellite observations provide reliable information about aerosol distributions and microphysical properties that can be used to improve radiative forcing estimates. Under some circumstances (e.g., over ocean), space-based measurements enable the distinction between natural and man-made aerosol signatures as long as they have different aerosols size distributions [Tanré *et al.*, 2001; Kaufman *et al.*, 2005] and that some information on their geographical origin is available. The largest amount of natural aerosols is composed of mineral dust and sea salt, which mostly contribute to the coarse mode whereas man-made aerosols mainly come from urban and industrial pollution, and man-made vegetation fires which are dominated by fine mode particles

(or accumulation mode) [Kaufman *et al.*, 2002]. Other aerosols mainly include volcanic dust, pollen, and carbonaceous aerosols from wild vegetation fires.

[3] Although elevated layers of aerosols are often transported above low-level clouds, most of aerosol properties retrievals from global remote sensing observations are limited to cloud-free scenes. On a regional scale, several approaches have been developed to quantify the direct effect of aerosols above clouds (AAC) [e.g., Chand *et al.*, 2009; De Graaf *et al.*, 2012; Meyer *et al.*, 2013]. Overlying absorbing aerosols have a warming effect due to the reduction of the local planetary albedo that is still poorly estimated. In addition to this direct effect, AAC such as biomass-burning aerosols may influence the dynamical evolution of cloud that might lead to a cloud top altitude reduction and a cloud thickening [Johnson *et al.*, 2004; Wilcox, 2010]. Moreover, above-cloud aerosols affect the retrieved values of the underlying cloud optical depth and effective radius [Haywood *et al.*, 2004; Wilcox *et al.*, 2009]. There is a lack of global observations about AAC loading and properties due to retrieval methods that are currently limited over space and time. In spite of the ability of a satellite-borne lidar like Cloud-Aerosol Lidar with Orthogonal Polarization to detect aerosol and cloud vertical structure [Chand *et al.*, 2008; Winker *et al.*, 2013], the current observations provide limited spatial coverage. Torres *et al.* [2012] and Jethva *et al.* [2013] have proved the ability of passive sensor to detect the presence of an aerosol layer above cloud and to quantify their amount as well as the cloud optical depth for some case studies. Multidirectional polarization measurements have also shown sensitivity to AAC scenes [Waquet *et al.*, 2009, 2013; Hasekamp, 2010; Knobelspiess *et al.*, 2011]: aerosols generate an additional polarized light at side scattering angles and reduce the polarized signal of the cloud-bow. In light of these observations and thanks to the A-Train, Polarization and Directionality of the Earth’s Reflectances (POLDER) measurements combined with collocated and simultaneous information about clouds from MODIS paved the way for the development of a retrieval technique of AAC properties on a global scale for a year of data. These results, coupled with the clear-sky product over ocean (both fine and coarse mode) [Herman *et al.*, 2005] and over land (fine mode only) [Deuzé *et al.*, 2001] provided by POLDER are analyzed in this study.

2. Methodology

[4] The operational algorithm proceeds as described by Waquet *et al.* [2013]. The “single-pixel method” allows the retrieval of the Aerosol Optical Thickness (AOT) above liquid clouds and an aerosol model is chosen from the seven models considered by the algorithm (six small spherical models for the fine mode with a complex refractive index

¹Laboratoire d’Optique Atmosphérique, CNRS-INSU – UMR8518, Université Lille 1, Lille, France.

²Goddard Space Flight Center, NASA, Greenbelt, Maryland, USA.

Corresponding author: F. Waquet, Laboratoire d’Optique Atmosphérique, CNRS-INSU – UMR8518, Université Lille 1, Villeneuve-d’Ascq, Lille, France. (fabien.waquet@univ-lille1.fr)

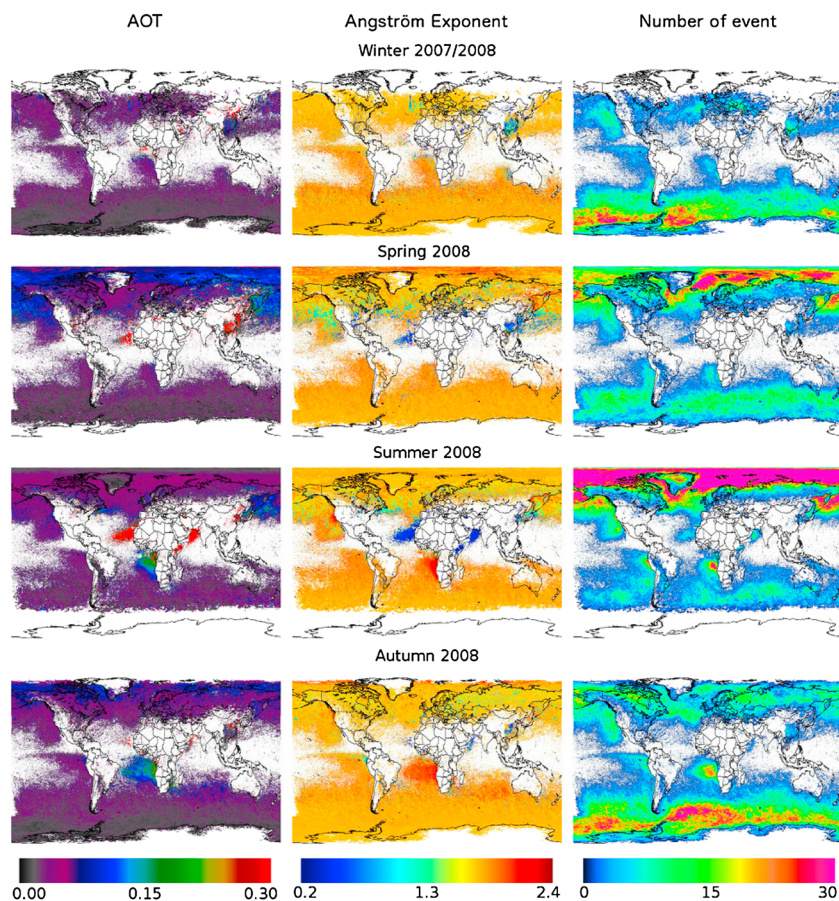


Figure 1. (left column) Global mean aerosol optical thickness at 865 nm, (middle column) mean Ångström exponent retrieved over clouds and (right column) number of retrievals in function of the season.

of 1.47–0.01 i for both wavelengths and one nonspherical coarse model for dust). The method consists of a comparison between POLDER measurements at 670 and 865 nm and precomputed polarized radiances with a successive order of scattering code [Deuzé *et al.*, 1989].

[5] It should be noted that discrimination between fine mode aerosols and dust particles becomes inaccurate at small AOT. As a consequence, we first estimate AOT by only considering the six fine mode particle models and exclude the dust model if the AOT retrieved at the first step is smaller than 0.1 at 865 nm.

[6] Several filters are then applied to enhance the quality of the product. Data that are not well-fitted to the models are rejected. Further, the variability of cloud properties (i.e., cloud optical depth and cloud droplet effective radius) within each POLDER pixel is evaluated from MODIS retrievals at higher resolution ($1 \times 1 \text{ km}^2$ at nadir) and only homogeneous pixels are kept [Waquet *et al.*, 2013]. The cloud optical thickness has to be larger than 3.0 to ensure the saturation of the polarized light scattered by the cloud layer. In order to avoid cirrus contamination, three additional criteria are added. The first one is based on the differences observed between the cloud top pressure provided by both MODIS (IR technique, [Menzel *et al.*, 2006]) and POLDER (Rayleigh [Goloub *et al.*, 1994] and O_2 [Vanbauce *et al.*, 2003] techniques). Second, the cloud phase index derived following Riedi *et al.* [2010] should not exceed 120, which corresponds to liquid clouds and “mixed-phase” clouds. The last criterion relies on a filter related to the brightness temperature

difference between the 8.6 and $11 \mu\text{m}$ MODIS bands. This filter ($\text{BTD}_{8-11} < -1.25 \text{ K}$) is introduced since it has shown an ability to distinguish dust from cirrus [Zhang *et al.*, 2006; Hansell *et al.*, 2007].

[7] Finally, data are aggregated from $6 \times 6 \text{ km}^2$ (POLDER native resolution at nadir) to $18 \times 18 \text{ km}^2$. We only keep the aggregated data for which the AOT standard deviation is smaller than 0.1 and that contain more than four $6 \times 6 \text{ km}^2$ POLDER pixels. This latter procedure allows to exclude cloud edges from the POLDER data.

3. Results

[8] The study focuses on the analysis of global AOT (at 865 nm) and Ångström exponent retrieved over clouds during 1 year (see Figures 1, left and 1, middle columns). We present average results for 3 month periods. The year is divided into four time periods: Winter (December 2007, January, and February 2008, see Figure 1, row 1); Spring (March, April, and May 2008, row 2); Summer (June, July, and August 2008, row 3) and Autumn (September, October, and November 2008, row 4). The Ångström Exponent (AE) is computed using the aggregated AOT at 865 nm and 670 nm for each AAC event with an AOT that is different from zero. Figure 1 shows the mean AE over 3 months (see Figure 1, middle column) as well as the number of retrievals (see Figure 1, right column).

[9] The global features displayed in Figure 1 show that the properties of the AAC vary with season and location. AAC

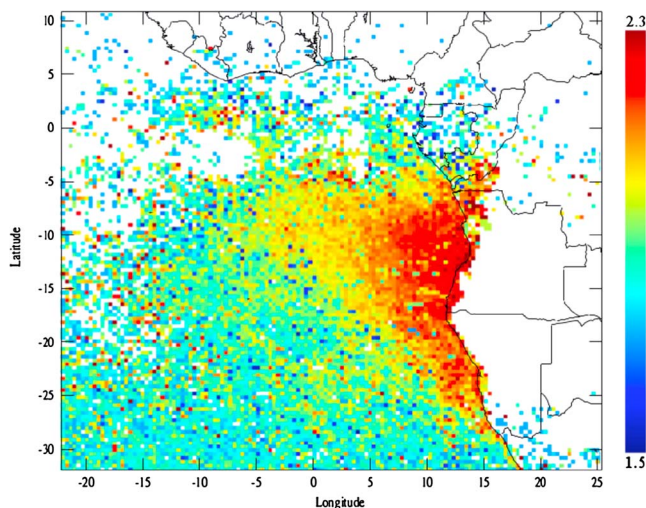


Figure 2. Ångström exponent retrieved above clouds by POLDER/PARASOL in the South Atlantic Ocean near South Africa. Mean values computed over 3 months (June, July, and August 2008).

retrievals are mainly located over ocean and downwind of continental sources. AAC retrievals with mineral dust particles are associated with the smallest values of AE. Fine mode AAC retrievals are associated with AOTs that mainly range between 0.1 and 0.2, knowing that fresh biomass-burning aerosols are related to AE larger than about 2.0. Values of AE of about 1 indicate regions influenced by both types of particles (i.e., mineral dust particles and fine mode particles).

[10] Africa is the main contributor to biomass-burning AAC retrievals. Man-made vegetation fires are frequently observed in Southern Africa between June and October, and meteorological processes favor biomass-burning aerosols transport to the west. During Summer, high mean AOT values (>0.2) associated with small particles are retrieved over a large area located over the tropical southeast Atlantic region. Persistent low-level clouds are present over these regions during Summer. The AAC occurrence is maximal for this season, with most retrievals detected off the coast of Angola (>30). The mean AOT patterns over this region are consistent with the ones obtained from previous regional studies [e.g., Chand *et al.*, 2009]. Our results also reveal that the properties of biomass-burning aerosols evolve during their transport above clouds. The mean AE progressively decreases from 2.5 to 1.7, from east to west (see Figure 2), which corresponds to an increase of $0.06 \mu\text{m}$ for the effective radius in our model database. This suggests that the mean size of the biomass-burning aerosols increases as they progressively move away from the South African coast and age. The transport of African biomass-burning aerosols above clouds over the Atlantic is also frequent during Autumn. A thick plume ($\text{AOT} > 0.15$) is observed crossing the South Atlantic, and almost reaching Brazil. The method also detects biomass-burning AAC events over southeast Africa and the Indian Ocean, near the coasts of South Africa and southeastern Mozambique. These AAC occurrences are observed in late August and increase in September and October, as the crop clearing fire season in Southern Africa progressively shifts from north to south. The AOT and AE maps also clearly show that biomass-burning aerosols originating from southern Africa can be transported above clouds

across the Indian Ocean over large distance as noted in earlier studies [e.g., Swap *et al.*, 2003; Stein *et al.*, 2003]. These biomass-burning aerosols are transported east due to the prevailing wind in this region and reach Australia.

[11] Asia is the second largest contributor of man-made AAC. Our results indicate that aerosol layers are transported above clouds across the North Pacific Ocean (35°N – 60°N) from Asia to the USA. This transport occurs during the spring and summer seasons. Persistent thick low-level clouds cover this region, and the number of AAC occurrences are significant, especially during the Spring. Many fine mode particles were detected since several AAC with significant AOT (>0.2) and AE of about 1.7 were observed, suggesting pollution aerosols (i.e., fine mode aerosols larger than biomass-burning aerosols). Our results also indicate that mineral dust particles are transported across the North Pacific. For instance, mean AE of about 1.0 are retrieved near the coasts of Japan during the Summer, and near the USA coast during the Spring. These results are consistent with previous studies showing transpacific Asian aerosol pollution and mineral dust transport occurring during the spring and summer, with a peak in Spring [Yu *et al.*, 2008]. The pollution aerosols originate from the Asian megalopolis, whereas the mineral dust particles originate from Mongolia and northeastern China deserts [Prospero *et al.*, 2002]. Fresh biomass-burning aerosols (AE > 2.0) are also detected over the Okhotsk Sea, near the Siberian coast for the Spring and Summer. These aerosols are emitted by wild fires that frequently occur over eastern Siberia. Our results indicate that these biomass-burning aerosols are also transported above clouds over the western North Pacific Ocean and are likely to contribute to the transpacific outflow.

[12] The retrievals detect many AAC events associated with fine mode aerosols over the North Pole between mid-April and mid-June. The arctic haze phenomenon is seasonal (mainly spring) and has man-made origin [Garrett and Verzella, 2008], which is consistent with our results. Our daily result also exhibit large AE values (>2.0) over this region, which indicates that biomass-burning aerosols are transported above clouds over the Arctic. Airborne measurements [Quennehen *et al.*, 2012] have shown that European air masses with biomass-burning aerosols and Asian air masses with contributions from both biomass-burning aerosols and pollution particles (with soot-like inclusion) were transported to the pole during Spring 2008. Sometimes the method also detected mineral dust AAC events over the Arctic in spring, and our results indicate that various types of aerosols that originated from eastern Asia (i.e., mineral dust and fine mode aerosols) contribute to the arctic haze.

[13] AAC events associated with fine mode particles are also detected in other regions, including Autumn over North America, North Russia, and near the west coast of Greenland. The method retrieves AE values of 1.7 for these AAC events, suggesting man-made aerosols. The nature of particles cannot be identified with confidence, since the AOT for these cases are generally small. The same type of AAC events were also detected over the North Atlantic, near the east coast of USA for the summer period. These aerosols may have originated from an industrial outflow from North America [Coddington *et al.*, 2010]. Biomass-burning AAC events are detected over a small area located over the southeast Asia (mainly over Vietnam and southern China) during the spring. These AAC events are related to man-made crop

Table 1. Mean Aerosol Optical Thickness and Number of Successful Retrievals Above Clouds and Clear-Sky (Ocean + Land) Scenes

Results/Periods	Winter	Spring	Summer	Autumn	Total for 2008
	<i>Fine mode particles^a</i>				
$\tau_{\text{clear_sky}}$	0.026	0.027	0.026	0.027	0.026
$\tau_{\text{all_sky}} (\tau_{\text{cloud}} \geq 0.00)$	0.026	0.033	0.032	0.031	0.031
$\tau_{\text{all_sky}} (\tau_{\text{cloud}} \geq 0.05)$	0.030	0.036	0.039	0.035	0.034
$\tau_{\text{all_sky}} (\tau_{\text{cloud}} \geq 0.10)$	0.028	0.033	0.031	0.032	0.031
$\tau_{\text{cloud}} (\tau_{\text{cloud}} \geq 0.00)$	0.026	0.051	0.048	0.045	0.041
$\tau_{\text{cloud}} (\tau_{\text{cloud}} \geq 0.05)$	0.085	0.105	0.099	0.096	0.097
$\tau_{\text{cloud}} (\tau_{\text{cloud}} \geq 0.10)$	0.145	0.159	0.167	0.162	0.161
$N_{\text{clear_sky}}$	11039831	13546657	14249989	13587873	52611076
$N_{\text{cloud}} (\tau_{\text{cloud}} \geq 0.00)$	5393916	4634317	5131051	5924123	21083407
$N_{\text{cloud}} (\tau_{\text{cloud}} \geq 0.05)$	855146	1755204	1713771	1688658	6012779
$N_{\text{cloud}} (\tau_{\text{cloud}} \geq 0.10)$	186726	633778	529621	489032	1839157
	<i>Mineral dust particles^b</i>				
τ_{cloud}	0.430	0.410	0.445	0.395	0.425
N_{cloud}	57746	132295	145217	64450	399708

^aMean aerosol optical thickness and number of successful retrievals above clouds and clear-sky (ocean + land) scenes for the fine mode particles. N is the number of aerosol retrievals and τ is the aerosol optical thickness at 865 nm. The suffixes “cloud” and “clear_sky” refer to aerosol retrievals performed above clouds and over clear-sky scenes, respectively. The total optical thickness, $\tau_{\text{all_sky}}$, is the mean aerosol optical thickness computed for all successful retrievals performed for each type of scenes.

^bMean aerosol optical thickness and number of aerosol retrievals estimated above clouds for mineral dust particles. The results shown in Table 1 include AOT retrievals equal to 0.

fires [Hsu *et al.*, 2003]. Some biomass-burning AAC events were also detected along the coast of California in June and July (see the AE maps for the Summer, $\text{AE} > 2.0$) originating from local vegetation wild fires that occurred in California during the summer 2008. These events however do not result in a strong signal in our seasonal mean AOT.

[14] Table 1 shows global mean results for AOT and the number of successful retrievals for the year 2008. We merged the aerosol products provided for the fine mode aerosols over ocean and land for clear-sky conditions with the ones retrieved above clouds. We computed an “all-sky” mean AOT that accounts for all successful retrievals performed for the three types of scenes. The method cannot identify with confidence the type of aerosols located above clouds for AOT smaller than 0.1. We then computed three estimates of this latter quantity by only considering fine mode AAC retrievals associated with (i) AOTs larger than 0.1, (ii) AOTs larger than 0.05, and (iii) by considering all fine mode AAC (see Table 1). The comparison of the clear-sky and all-sky mean AOTs shows that accounting for AAC retrievals increases the global mean AOT for fine mode aerosols by 25(±6)% for the year 2008.

[15] The AE maps reveal four main regions with mineral dust above clouds: the tropical North East Atlantic region close to the Sahara, the Arabian sea, the southeastern part of the horn of Africa (mostly Ethiopia and Somalia), and the southeastern part of Asia. To a lesser extent, AAC events with mineral dust particles are also detected over northern Iran during the spring period and near the west coast of Australia during the boreal winter period. Mineral dust AAC is associated with a small number of events and large mean values of AOT (see Table 1). The transport of mineral dust particles above clouds is frequent over the south and east parts of Asia, throughout the year, with a maximum in spring. The other regions mainly show AAC events for the summer period. The transport of Saharan mineral dust is frequent across the Atlantic Ocean, and mineral dust particles are often transported above low-level clouds near the coasts of North Africa [Herman *et al.*, 1997; Haywood *et al.*, 2003]. Our methodology detects a large mineral dust plume extending over the tropical North East Atlantic between the

African coast (12–14° in latitudes) and the middle of the Atlantic Ocean. The method retrieves mean AOT values between 0.3 and 0.9, with the maximal mean AOT retrieved near the coast of Mauritania. The main source areas for the Arabian Sea region could be the surrounding deserts located in Oman and in the Arabian Peninsula [Prospero *et al.*, 2002], whereas the mineral dust AAC observed over the horn of Africa could be originating from local sources previously detected in Ethiopia and Somalia [Léon and Legrand, 2003]. The analysis detects a dust plume over the middle of the North Atlantic Ocean during the winter period; AAC events with mineral dust particles are also detected along the northeastern coast of the USA (AE of about 1.0) for the summer and spring periods and over the Gulf of Mexico for the spring period. We assume that these particles were transported from North Africa since the long range transport of Saharan dust is frequent over the North Atlantic Ocean.

4. Conclusion

[16] This study shows that the amount of man-made and natural aerosols transported above clouds is significant at the global scale. Current operational aerosol retrievals from passive sensors are restricted to cloud-free scenes and therefore significantly underestimate the total amount of aerosols. A positive above-cloud radiative forcing is typically expected when absorbing particles, such as biomass-burning aerosols, that are present above clouds though the magnitude (as well as the sign) depends on AOT, aerosol spectral single scattering albedo, and cloud optical thickness [e.g., Keil and Haywood, 2003]. Our results indicate that a significant amount of such particles are transported above clouds in various regions of the world, including the North Pole during the Spring which was not expected. As previously mentioned, imager retrieved cloud property biases (primarily optical thickness and derived water path) are also expected when biomass-burning aerosols and mineral dust particles are present above clouds, and precautions should be therefore taken when analyzing cloud retrievals in regions where such AAC events are now identified. Another interesting point is the fact that our method does not retrieve significant AOT over clouds in cloudy region located

far away from continental sources, such as the Antarctic Ocean, as it might be expected. The use of a limited number of aerosol models and the lack of sensitivity to mineral dust particles, when the aerosol optical thicknesses above clouds become small, are two limitations that could be overcome by using a more sophisticated retrieval method [e.g., Waquet et al., 2013]. We also note that our method is currently restricted to AAC scenes with cloud optical thickness larger than 3.0 and homogeneous liquid water clouds. The results presented in this study therefore might still underestimate slightly the total number of AAC events. However, the above-cloud direct aerosol radiative effect increases with cloud optical thickness, so that AAC events identified in this study are the most important for estimating the radiative effect on a global scale.

[17] **Acknowledgments.** This work has been supported by the Programme National de Télédétection Spatiale (PNTS, <http://www.insu.cnrs.fr/actions-sur-projets/pnts-programme-national-de-teledetection-spatiale>), grant n° PNTS-2013-10. The authors are grateful to CNES, NASA, and the ICARE data and services center.

[18] The Editor thanks two anonymous reviewers for their assistance in evaluating this paper.

References

- Chand, D., T. L. Anderson, R. Wood, R. J. Charlson, Y. Hu, Z. Liu, and M. Vaughan (2008), Quantifying above-cloud aerosol using spaceborne lidar for improved understanding of cloudy-sky direct climate forcing, *J. Geophys. Res.*, *113*, D13206, doi:10.1029/2007JD009433.
- Chand, D., R. Wood, T. L. Anderson, S. K. Satheesh, and R. J. Charlson (2009), Satellite-derived direct radiative effect of aerosols dependent on cloud cover, *Nat. Geosci.*, *2*(3), 181–184, doi:10.1038/ngeo437.
- Coddington, O. M., P. Pilewskie, J. Redemann, S. Platnick, P. B. Russell, K. S. Schmidt, W. J. Gore, J. Livingston, G. Wind, and T. Vukicevic (2010), Examining the impact of overlying aerosols on the retrieval of cloud optical properties from passive remote sensing, *J. Geophys. Res.*, *115*, D10211, doi:10.1029/2009JD012829.
- De Graaf, M., L. G. Tilstra, P. Wang, and P. Stammes (2012), Retrieval of the aerosol direct radiative effect over clouds from spaceborne spectrometry, *J. Geophys. Res.*, *117*, D07207, doi:10.1029/2011JD017160.
- Deuzé, J. L., M. Herman, and R. Santer (1989), Fourier series expansion of the transfer equation in the atmosphere-ocean system, *J. Quant. Spectrosc. Radiat. Transfer*, *41*(6), 483–494, doi:10.1016/0022-4073(89)90118-0.
- Deuzé, J. L., et al. (2001), Remote sensing of aerosols over land surfaces from POLDER-ADEOS-1 polarized measurements, *J. Geophys. Res.*, *106*, 4913–4926, doi:10.1029/2000JD900364.
- Garrett, T. J., and L. L. Verzella (2008), Looking back: An evolving history of Arctic aerosols, *Bull. Am. Meteorol. Soc.*, *89*, 299–302, doi:10.1175/BAMS-89-3-299.
- Goloub, P., J.-L. Deuzé, M. Herman, and Y. Fouquart (1994), Analysis of the POLDER polarization measurements performed over cloud covers, *IEEE Trans. Geosci. Remote Sens.*, *32*, 78–88.
- Hansell, R. A., S. C. Ou, K. N. Liou, J. K. Roskovensky, S. C. Tsay, C. Hsu, and Q. Ji (2007), Simultaneous detection/separation of mineral dust and cirrus clouds using MODIS thermal infrared window data, *Geophys. Res. Lett.*, *34*, L11808, doi:10.1029/2007GL029388.
- Hasekamp, O. P. (2010), Capability of multi-viewing-angle photo-polarimetric measurements for the simultaneous retrieval of aerosol and cloud properties, *Atmos. Meas. Tech. Discuss.*, *3*(2), 1229–1262, doi:10.5194/amt-d-1229-2010.
- Haywood, J. M., S. R. Osborne, P. Francis, M. Glew, N. Loeb, E. Highwood, D. Tanré, G. Myhre, P. Formenti, and E. Hirst (2003), Radiative properties and direct radiative effect of Saharan dust measured by the C-130 aircraft during SHADE: 1. Solar spectrum, *J. Geophys. Res.*, *108*(D18), 8577, doi:10.1029/2002JD002687.
- Haywood, J. M., S. R. Osborne, and S. J. Abel (2004), The effect of overlying absorbing aerosol layers on remote sensing retrievals of cloud effective radius and cloud optical depth, *Q. J. R. Meteorol. Soc.*, *130*(598), 779–800, doi:10.1256/qj.03.100.
- Herman, J. R., P. K. Bhartia, O. Torres, C. Hsu, C. Sefor, and E. Celarier (1997), Global distribution of UV-absorbing aerosols from Nimbus 7/TOMS data, *J. Geophys. Res.*, *102*, 16,911–16,922.
- Herman, M., J.-L. Deuzé, A. Marchand, B. Roger, and P. Lallart (2005), Aerosol remote sensing from POLDER/ADEOS over the ocean: Improved retrieval using a nonspherical particle model, *J. Geophys. Res.*, *110*, D10S02, doi:10.1029/2004JD004798.
- Hsu, N. C., J. R. Herman, and S.-C. Tsay (2003), Radiative impacts from biomass burning in the presence of clouds during boreal spring in Southeast Asia, *Geophys. Res. Lett.*, *30*(5), 1224, doi:10.1029/2002GL016485.
- Jethva, H., O. Torres, L. A. Remer, and P. K. Bhartia (2013), A color ratio method for simultaneous retrieval of aerosol and cloud optical thickness of above-cloud absorbing aerosols from passive sensors: Application to MODIS measurements, *IEEE Trans. Geosci. Remote Sens.*, *51*, 3862–3870, doi:10.1109/TGRS.2012.2230008.
- Johnson, B. T., K. P. Shine, and P. M. Forster (2004), The semi-direct aerosol effect: Impact of absorbing aerosols on marine stratocumulus, *Q. J. R. Meteorol. Soc.*, *130*(599), 1407–1422, doi:10.1256/qj.03.61.
- Kaufman, Y. J., D. Tanré, and O. Boucher (2002), A satellite view of aerosols in the climate system, *Nature*, *419*(6903), 215–223, doi:10.1038/nature01091.
- Kaufman, Y. J., O. Boucher, D. Tanré, M. Chin, L. A. Remer, and T. Takemura (2005), Aerosol anthropogenic component estimated from satellite data, *Geophys. Res. Lett.*, *32*, L17804, doi:10.1029/2005GL023125.
- Keil, A., and J. M. Haywood (2003), Solar radiative forcing by biomass burning aerosol particles during SAFARI 2000: A case study based on measured aerosol and cloud properties, *J. Geophys. Res.*, *108*(D13), 8467, doi:10.1029/2002JD002315.
- Knobelspiess, K., B. Cairns, J. Redemann, R. W. Bergstrom, and A. Stohl (2011), Simultaneous retrieval of aerosol and cloud properties during the MILAGRO field campaign, *Atmos. Chem. Phys. Discuss.*, *11*(2), 6363–6413, doi:10.5194/acpd-11-6363-2011.
- Léon, J.-F., and M. Legrand (2003), Mineral dust sources in the surroundings of the north Indian Ocean, *Geophys. Res. Lett.*, *30*(6), 1309, doi:10.1029/2002GL016690.
- Menzel, W. P., R. A. Frey, B. A. Baum, and H. Zhang (2006), *Cloud Top Properties and Cloud Phase Algorithm Theoretical Basis Document, Version 7*, 55 pp. [Available online at: <http://modisatmos.gsfc.nasa.gov/docs/MOD06CT:MYD06CTATBDC005.pdf>, last access: August 2012].
- Meyer, K., S. Platnick, L. Oreopoulos, and D. Lee (2013), Estimating the direct radiative forcing of absorbing aerosols overlying marine boundary layer clouds in the southeast Atlantic using MODIS and CALIOP, *J. Geophys. Res. Atmos.*, *118*, 4801–4815, doi:10.1002/jgrd.50449.
- Prospero, J. M., P. Ginoux, O. Torres, S. E. Nicholson, and T. E. Gill (2002), Environmental characterization of global sources of atmospheric soil dust identified with the NIMBUS 7 Total Ozone Mapping Spectrometer (TOMS) absorbing aerosol product, *Rev. Geophys.*, *40*(1), 1002, doi:10.1029/2000RG000095.
- Quennehen, B., A. Schwarzenboeck, A. Matsuki, J. F. Burkhart, A. Stohl, G. Ancellet, and K. S. Law (2012), Anthropogenic and forest fire pollution aerosol transported to the Arctic: Observations from the POLARCAT-France spring campaign, *Atmos. Chem. Phys.*, *12*, 6437–6454, doi:10.5194/acp-12-6437-2012.
- Ramanathan, V., P. J. Crutzen, J. T. Kiehl, and D. Rosenfeld (2001), Aerosols, climate, and the hydrological cycle, *Science (New York, N.Y.)*, *294*(5549), 2119–2124, doi:10.1126/science.1064034.
- Riedi, J., B. Marchant, S. Platnick, B. A. Baum, F. Thieuleux, C. Oudard, F. Parol, J.-M. Nicolas, and P. Dubuisson (2010), Cloud thermodynamic phase inferred from merged POLDER and MODIS data, *Atmos. Chem. Phys.*, *10*, 11,851–11,865, doi:10.5194/acp-10-11851-2010.
- Stein, D. C., R. J. Swap, S. Greco, S. J. Piketh, S. A. Macko, B. G. Doddridge, T. Elias, and R. T. Bruinjes (2003), Haze layer characterization and associated meteorological controls along the eastern coastal region of southern Africa, *J. Geophys. Res.*, *108*(D13), 8506, doi:10.1029/2002JD003237.
- Swap, R. J., H. J. Annegarn, J. T. Suttles, M. D. King, S. Platnick, J. L. Privette, and R. J. Scholes (2003), Africa burning: A thematic analysis of the Southern African Regional Science Initiative (SAFARI 2000), *J. Geophys. Res.*, *108*(D13), 8465, doi:10.1029/2003JD003747.
- Tanré, D., F. M. Bréon, J. L. Deuzé, M. Herman, P. Goloub, F. Nadal, and A. Marchand (2001), Global observation of anthropogenic aerosols from satellite, *Geophys. Res. Lett.*, *28*, 4555–4558, doi:10.1029/2001GL013036.
- Torres, O., J. Hiren, and P. K. Bhartia (2012), Retrieval of aerosol optical depth above clouds from OMI observations, sensitivity analysis and case studies, *J. Atmos. Sci.*, *69*, 1037–1053, doi:10.1175/JAS-D-11-0130.1.
- Vanbauce, C., B. Cadet, and R. T. Marchand (2003), Comparison of POLDER apparent and corrected oxygen pressure to ARM/MMCR cloud boundary pressures, *Geophys. Res. Lett.*, *30*(5), 1212, doi:10.1029/2002GL016449.
- Waquet, F., J. Riedi, L. C. Labonnote, P. Goloub, B. Cairns, J.-L. Deuzé, and D. Tanré (2009), Aerosol remote sensing over clouds using the A-Train observations, *J. Atmos. Sci.*, *66*, 2468–2480, doi:10.1175/2009JAS3026.1.
- Waquet, F., et al. (2013), Retrieval of aerosol microphysical and optical properties above liquid clouds from POLDER/PARASOL polarization measurements, *Atmos. Meas. Tech.*, *6*, 991–1016, doi:10.5194/amt-6-991-2013.
- Wilcox, E. M. (2010), Stratocumulus cloud thickening beneath layers of absorbing smoke aerosol, *Atmos. Chem. Phys.*, *10*(23), 11,769–11,777.
- Wilcox, E. M., Harshvardhan, and S. Platnick (2009), Estimate of the impact of absorbing aerosol over cloud on the MODIS retrievals of

- cloud optical thickness and effective radius using two independent retrievals of liquid water path, *J. Geophys. Res.*, *114*, D05210, doi:10.1029/2008JD010589.
- Winker, D. M., J. L. Tackett, B. J. Getzewich, Z. Liu, M. A. Vaughan, and R. R. Rogers (2013), The global 3-D distribution of tropospheric aerosols as characterized by CALIOP, *Atmos. Chem. Phys.*, *13*(6), 3345–3361.
- Yu, H., L. A. Remer, M. Chin, H. Bian, R. G. Kleidman, and T. Diehl (2008), A satellite-based assessment of transpacific transport of pollution aerosol, *J. Geophys. Res.*, *113*, D14S12, doi:10.1029/2007JD009349.
- Zhang, P., N. Lu, X. Hu, and C. Dong (2006), Identification and physical retrieval of dust storm using three MODIS thermal IR channels, *Global Planet. Change*, *52*(1–4), 197–206, doi:10.1016/j.gloplacha.2006.02.014.